AIAA 80-0455R

Influence of Wing, Fuselage, and Tail Design on Rotational Flow Aerodynamics Beyond Maximum Lift

William Bihrle Jr.*
Bihrle Applied Research, Inc., Jericho, N.Y.
and
James S. Bowman Jr.†
NASA Langley Research Center, Hampton, Va.

The NASA Langley Research Center has initiated a broad general aviation stall/spin research program. A rotary balance system was developed to support this effort. This system, located in the Langley spin tunnel, makes it possible to identify airplane aerodynamic characteristics in a rotational flow environment, and thereby permits prediction of spins. This paper presents a brief description of the experimental setup, testing technique, five model programs conducted to date, and an overview of the rotary balance results and their correlation with spin tunnel free-spinning model results. It is shown, for example, that there is a pronounced nonlinear dependency of the aerodynamic moments on rotational rate and that these moments are very configuration dependent. Fuselage shape, horizontal tail, and, in some instances, wing location are shown to appreciably influence the yawing moment characteristics above an angle of attack of 45 deg.

Nomenclature

b = wing span
B = body
$\bar{c}$ = mean aerodynamic chord
i_s = incidence of horizontal tail, positive when trailing edge is down
V = freestream velocity
V' = vertical tail
W = wing
α = angle of attack
β = angle of sideslip
Ω = angular velocity about spin axis
$\Omega b/2V$ = spin coefficient, positive for clockwise spin

Introduction

THE NASA Langley Research Center has initiated a broad general aviation stall/spin research program which includes spin tunnel and free-flight radio control model tests, as well as full-scale flight tests, for a number of configurations typical of light, general aviation airplanes. To support these free-flight investigations, a rotary balance was developed for the Langley spin tunnel to rapidly identify airplane aerodynamic characteristics in a rotational flow environment. The influence of spin radius, angle of attack, sideslip angle, rate of rotation, and control settings on the aerodynamics can be measured, thereby permitting prediction of incipient and developed spin characteristics. This information is being obtained for the configurations being flown in the stall/spin research program in order to establish a data base for analysis of model and full-scale flight results, and to develop design charts for desirable stall/spin characteristics.

This paper presents a brief description of the experimental setup, testing technique, model programs conducted to date, and an overview of the rotary balance results and their correlation with free-spinning model results. The importance of wing, horizontal tail location, and fuselage shape in determining developed spin characteristics is documented herein for the first time.

Rotary Balance Apparatus

Background

A rotary balance is used to measure forces and moments acting on an airplane while subjected to rotational flow conditions. The need for these data was recognized early in aircraft development. For example, early researchers noted in 1928[1] that the use of "straight" force tests conduce to erroneous conclusions when applied to the spin. NACA investigators at that time developed a "spinning" balance[2] installed in a 5-ft vertical tunnel; they reasoned that subjecting all components of an airplane model to a constant velocity vector during static force tests was an unsatisfactory simulation of flow conditions existing in a spin.

This concern is certainly warranted relative to today's general aviation airplane designs. Their spins are characterized by high values of $\Omega b/2V$.‡ (This is due to high rates of rotation and low rates of descent.) Hence a difference of up to 80-deg in angle of attack between wing tips, and a 60-deg difference in sideslip angle between the nose and tail can be realized in a flat spin.

The early NACA "spinning" balance's usefulness was limited by model and tunnel size. Also, forces and moments were measured by an externally mounted six-component balance that was large relative to the model. Consequently, by 1945, a "rotary" balance was developed[3] for the Langley 20-ft spin tunnel. Because of limited instrumentation then available, an inordinate amount of time and effort was needed to obtain a very small amount of data which was not repeatable. Hence, the rotary balance's use was soon abandoned for an appreciable period of time.

In recent years, NASA installed a rotary balance apparatus in the Langley full-scale tunnel and sponsored studies[4,5] to determine the ability of current analytical techniques to com-

Presented as Paper 80-0455 at the AIAA 11th Aerodynamic Testing Conference, Colorado Springs, Colo., March 18-20, 1980; submitted March 18, 1980; revision received April 27, 1981.

*President. Associate Fellow AIAA.
†Aerospace Technologist. Associate Fellow AIAA.

‡Rates of rotation have been traditionally expressed nondimensionally in terms of the linear and angular velocities V and Ω, respectively, and half the wing span. Thus the expression $\Omega b/2V$ is the ratio of the wing tip speed to the forward speed and is analogous to the arc tangent of the helix angle at the wing tip.

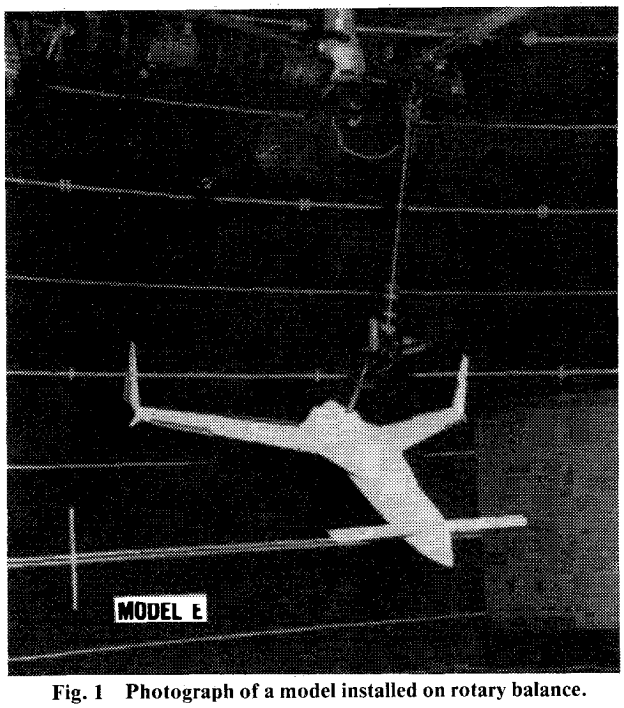

Fig. 1 Photograph of a model installed on rotary balance.

pute the flight motions of current fighter configurations. These studies clearly demonstrated the need to model the effects of spin rotation rate on the aerodynamic characteristics in all phases of the spinning motion. As a result of these experimental and analytical efforts, NASA subsequently modernized the rotary balance installed in the spin tunnel. The data discussed herein was obtained with this updated apparatus.

Test Equipment

A photograph and sketch of the rotary balance apparatus installed in the Langley spin tunnel are shown in Figs. 1 and 2, respectively. The system's rotary arm, which rotates about a vertical axis at the tunnel center, is supported by a horizontal boom and is driven by a motor mounted external to the test section.

The test model is mounted on a strain gage balance which is affixed to the bottom of the rotary balance apparatus. Controls located outside the tunnel are used to activate motors on the rig, which position the model to the desired attitude. The angle-of-attack range of the rig is 0-90 deg and the sideslip angle range is ± 15 deg. Spin radius and lateral displacement motors allow the operator to position the moment center of the balance on the spin axis or at a specific distance from the spin axis. (This is done for each combination of angle of attack and sideslip angle.) It is customary to mount the balance moment center at the location about which the aerodynamic moments are desired. Electrical current from the balance, and to the motors on the rig, is conducted through slip-rings located at the rig head. Figure 2 shows examples of how the rig is positioned for different angles of attack and sideslip angles.

The model can be rotated up to 90 rpm in either direction. A range of $\Omega b/2V$ values can be obtained by adjusting rotational speed and/or tunnel airflow velocity. (Static aerodynamic forces and moments are, of course, obtained when $\Omega = 0$.)

A NASA six-component strain gage balance, mounted inside the model, is used to measure the normal, lateral, and longitudinal forces, and the yawing, rolling, and pitching moments acting about the model body axis.

The data acquisition, reduction, and presentation system is composed of a 12-channel scanner/voltmeter, a minicomputer, a plotter, and a CRT display. This equipment permits

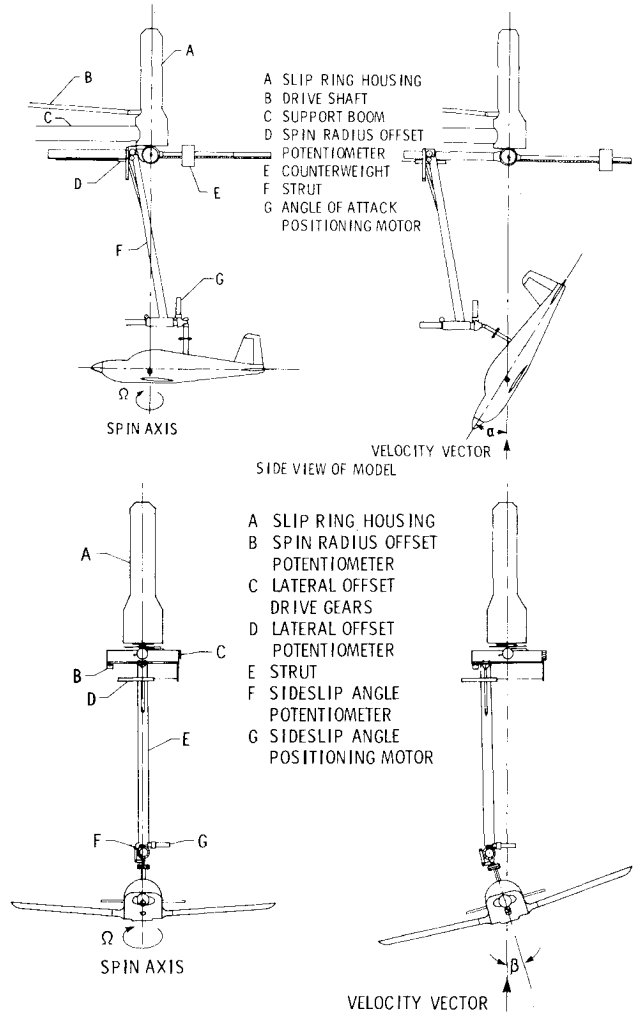

Fig. 2 Sketch of rotary balance.

data to be presented via on-line digital printouts and/or graphical plots.

Test Procedures

Rotary aerodynamic data are obtained in two steps.

The first step is to record the inertial forces and moments (tares) acting on the model at different attitudes and rotational speeds. To accomplish this, the model is enclosed in a sealed spherical structure which rotates with the model without touching it. Thus, the air immediately surrounding the model is rotated with it. As the rig is rotated at the desired attitude and rate, the inertial forces and moments generated by the model are measured and stored on magnetic tape for later use.

The second step is to record force and moment data with the air on and with the enclosure removed. Then the tares are subtracted from these data, leaving only the aerodynamic forces and moments, which are converted to coefficient form and stored on magnetic tape.

Model Programs

The five models shown in Figs. 1 and 3 have been tested and the six-component data have been published.[6-13] (Data for model D is to be published in 1981.) Models A, B, C, and D were deemed representative of single-engine general aviation configurations. The models had wing spans of approximately six feet and weighed twelve pounds or less. They were fabricated such that airplane components, horizontal tail, and wing (high or low) locations, as well as wing leading-edge

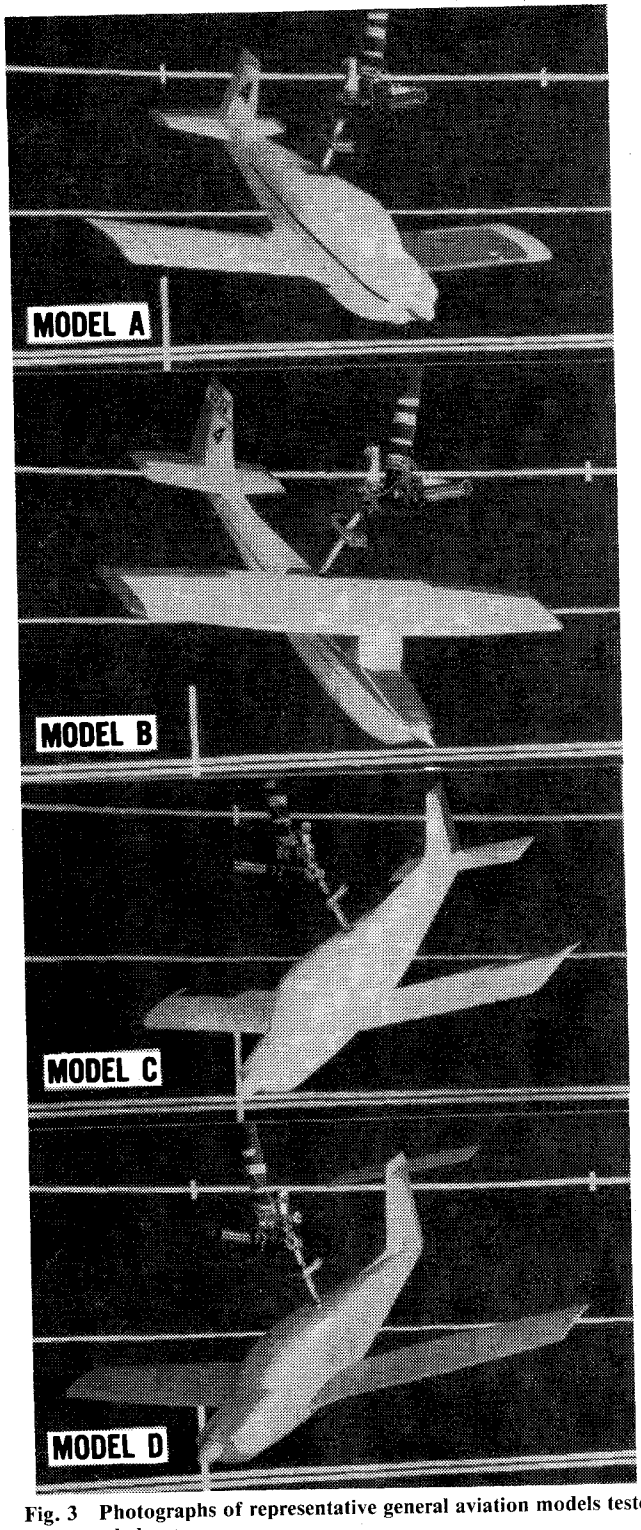

Fig. 3 Photographs of representative general aviation models tested on rotary balance.

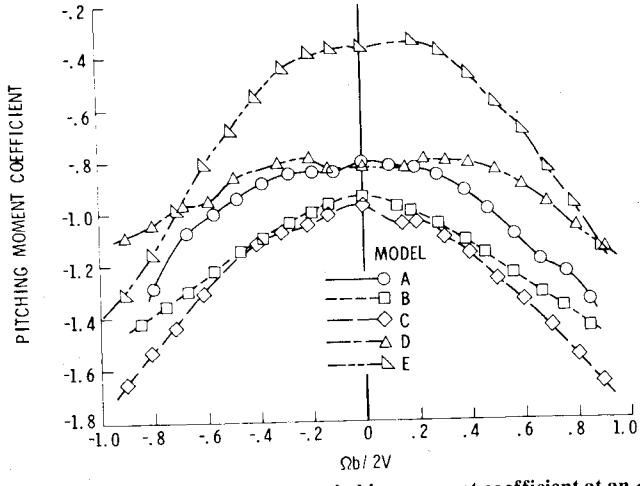

Fig. 4 Effect of rotation rate on pitching moment coefficient at an α of 60 deg for different airplane configurations.

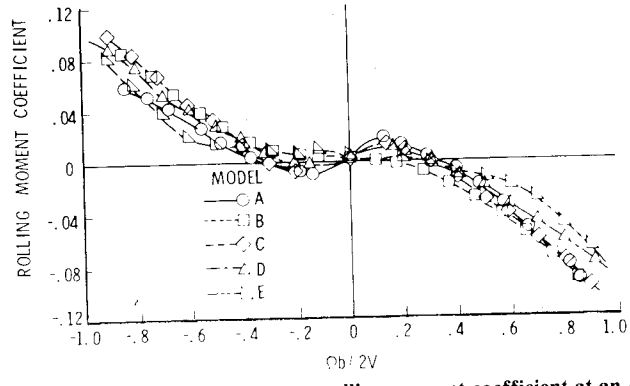

Fig. 5 Effect of rotation rate on rolling moment coefficient at an α of 50 deg for different airplane configurations.

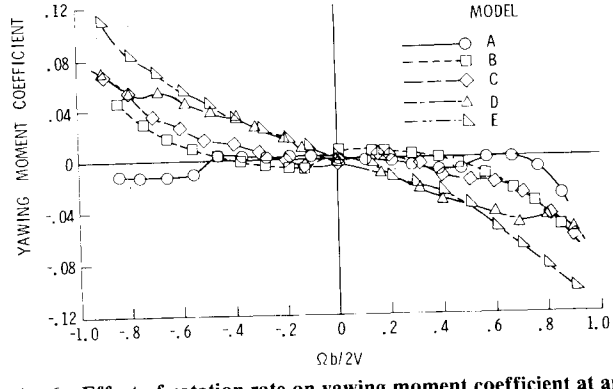

Fig. 6 Effect of rotation rate on yawing moment coefficient at an α of 60 deg for different airplane configurations.

shapes could be investigated. Provisions were also made for attaching various fuselage modifications and for setting different control deflections.

All of the configurations were tested through an angle-of-attack range of 8-90 deg at a zero sideslip angle. For angles of attack above 30 deg, the spin axis passed through the nominal airplane center of gravity location. For angles of attack below 35 deg, the spin axis was set to pass through the airplane nose. At each spin attitude, measurements were obtained for nominal $\Omega b/2V$ values of 0.1, 0.2, 0.3, 0.4, 0.5, 0.6, 0.7, 0.8, and 0.9 in both clockwise and counterclockwise directions, as well as for $\Omega b/2V = 0$ (static value). Selected configurations were also tested at $\beta = 10$ deg.

Data Presentation

The rotary balance data presented in this paper are for neutral control deflections, zero sideslip angle, and zero spin radius. Most of the data are presented for an α of 60 deg, since it is highly representative of the aerodynamic characteristics obtained above an α of 45 deg and, consequently, of the aerodynamics involved in a flat spin. Most of the data presented involves the yawing moment about the body axis, since it is the major contributor to the autorotative moment experienced in the flat spin (whereas, for steep spins in the 25-40 deg α range, autorotative rolling moments are the major driving element).

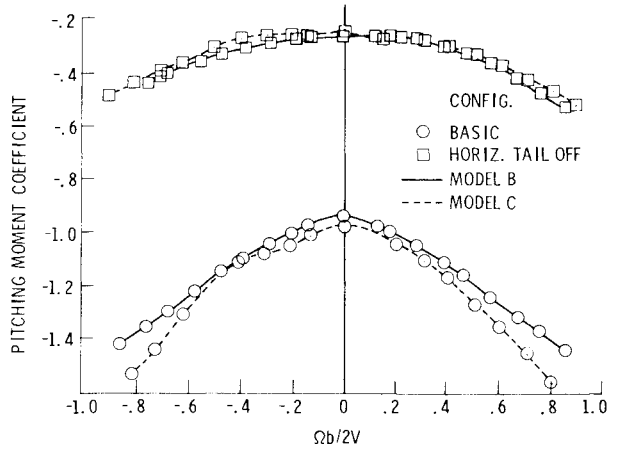

Fig. 7 Contribution of horizontal tail to pitching moment coefficient for models B and C.

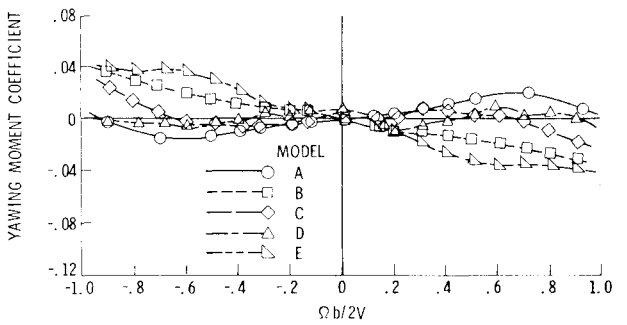

Fig. 8 Yawing moment characteristics at an α of 60 deg attributable to the bodies of the airplane configurations investigated.

The moment coefficients are presented in this paper as functions of the spin coefficient, $\Omega b/2V$. Positive values of $\Omega b/2V$ signify a clockwise (right) spin. In a right spin, positive rolling or yawing moments are autorotative (driving rather than damping moments). Conversely, negative rolling or yawing moments are autorotative for negative values of $\Omega b/2V$ (left spin).

Importance of Rotational Flow

The pronounced nonlinear dependency of the aerodynamic moments on rotational rate at a constant α value can be seen for different airplane models in Figs. 4-6. Figure 4 shows that pitching moment obtained in a rotational flow can be 50% or more greater than the static value. This pitching moment variation with rotational rate is mostly attributable to the horizontal tail at high α, as shown in Fig. 7. Figures 5 and 6 show that the sense of the rolling and yawing moments can change from autorotative to damping as a function of rotation rate. The rolling moment's dependency on rotational rate, even at an angle of attack of 50 deg, merits attention. All of these data illustrate the futility of computing spin equilibrium conditions without rotary balance data.

Influence of Airplane Components on Yawing Moment Characteristics

Since the moment characteristics at spinning attitudes were shown to be configuration dependent, the contribution various airplane components had on these characteristics was investigated. For the reasons given in the section entitled Data Presentation, the following discussion confines itself to the yawing moment.

Influence of Body

Figure 8 shows that the bodies of models A, B, C, D, and E have significantly different yawing moment characteristics. A body may be either autorotative or damped throughout the range of $\Omega b/2V$ values investigated, or it may vary between these characteristics as a function of spin rate. It is indicated, therefore, that the yawing moment characteristics shown in Fig. 6 were significantly influenced by the body shape associated with these models. As expected, the body and total configuration yawing moment characteristics presented in Figs. 8 and 6, respectively, are not identical, indicating the influence of other airplane components, such as the wing and tail surfaces. The influence of the body, consisting of a nose and a fuselage section, was, therefore, briefly examined in the presence of common wing and tail surfaces. This was accomplished by mounting the bodies of A and C over the body of model B, as shown in Fig. 9. By comparing the data for bodies A, B, and C presented in Fig. 10, it can be seen that, even in the presence of common wing and tail surfaces, the body can appreciably influence the overall airplane yawing moment characteristic.

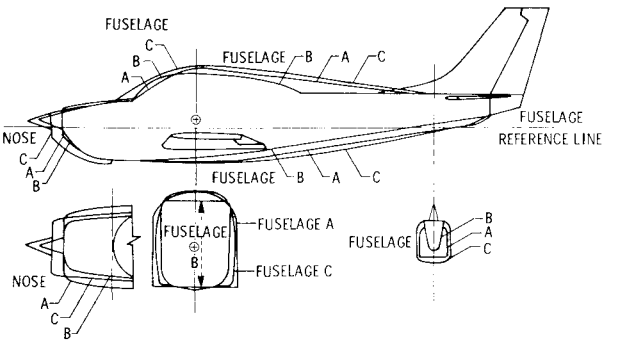

Fig. 9 Sketch of interchangeable noses and fuselages tested on model B.

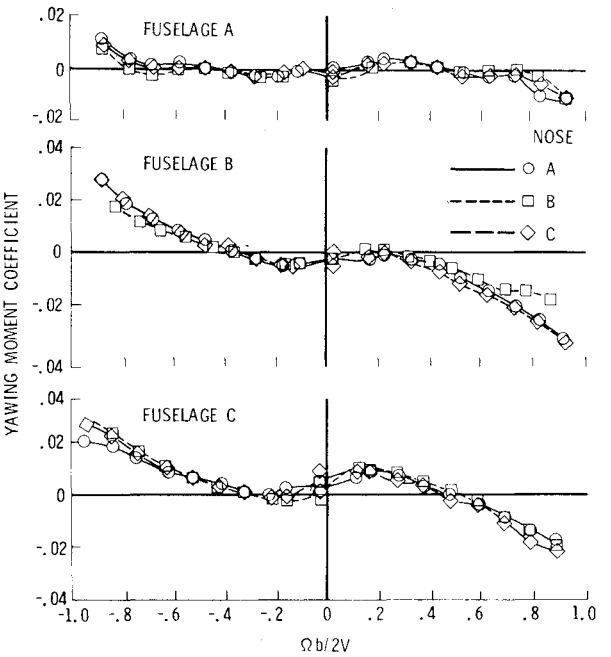

Fig. 10 Effect of interchanging nose shapes on fuselages A, B, and C relative to yawing moment characteristics at an α of 60 deg for common wing and tail surfaces.

Influence of Nose

The relative importance of nose shape on the body yawing moment characteristics in the presence of common wing and tail surfaces was also investigated. This was accomplished by testing the noses of models A, B, and C on each fuselage, as shown in Fig. 9. It was found that the various nose shapes and nose/fuselage volume ratios had no significant influence (see Fig. 10) on the yawing moment characteristics.

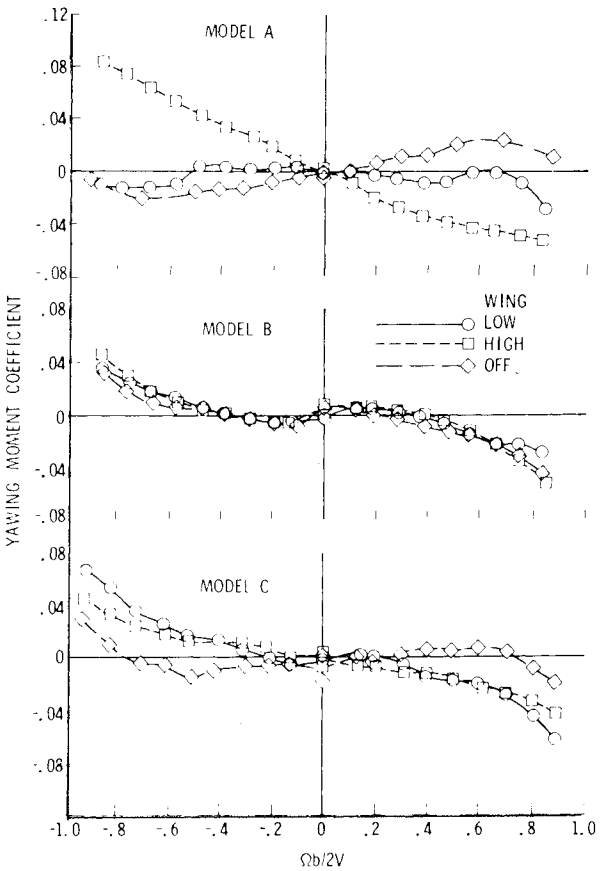

Fig. 11 Influence of wing on yawing moment characteristic at an α of 60 deg for models A, B, and C.

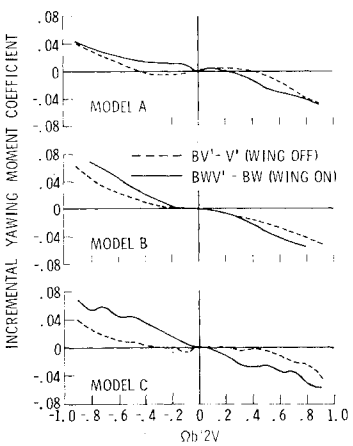

Fig. 12 Influence of wing on vertical tail effectiveness at an α of 60 deg for models A, B, and C when the horizontal tail is off.

Influence of Wing

Figure 11 shows the effect of the wing position (high or low), or its absence, on the yawing moment characteristics for models A, B, and C. It can be seen that the wing had an appreciably favorable influence on the yawing moment characteristics for models A and C, and none for model B. Also, whereas the location of the wing was not particularly significant for model C, a high wing location for model A was considerably more beneficial than was the low location. These results would indicate that the wing modifies the pressure distribution of the fuselage and, consequently, its contribution to the yawing moment. The existence and degree of beneficial wing interference is dictated by the fuselage shape.

The wing also appears to have a beneficial effect on the vertical tail effectiveness. This is illustrated in Fig. 12 for models A, B, and C, which presents the incremental yawing moment contribution of the vertical tail in and out of the presence of the wing (the horizontal tail being off in both instances). For all the models, the damping effect of the vertical tail is increased in the presence of the wing.

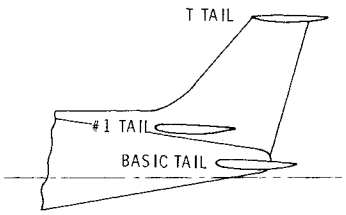

Fig. 13 Tail configurations tested on model C.

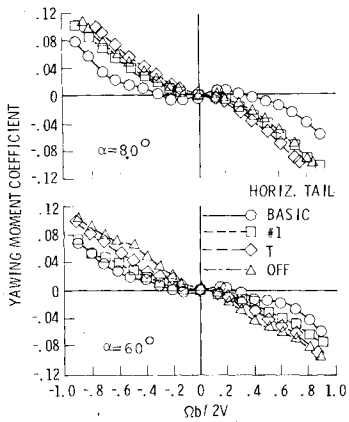

Fig. 14 Influence of horizontal tail location on yawing moment characteristic for model C.

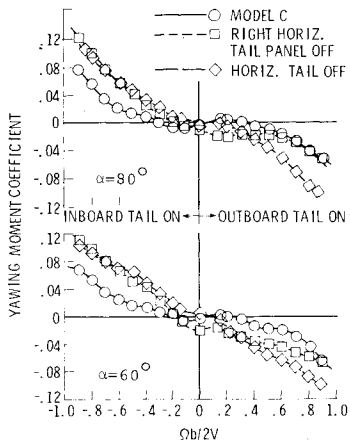

Fig. 15 Influence of outboard and inboard horizontal tail panel on yawing moment characteristic for model C.

Influence of Horizontal Tail

The horizontal tail influence on the yawing moment characteristics demonstrated herein at an α of 60 and 80 deg with model C is applicable to models A, B, and D as well.

The yawing moment characteristics for the three horizontal tail locations shown in Fig. 13 are presented in Fig. 14. It can be seen that the horizontal tail location can significantly degrade configuration damping characteristics. In this respect, the T-tail configuration is the most desirable of the three tested, since it approximates the horizontal tail-off case.

Component tests conducted during these investigations demonstrated that the vertical tail contribution to yaw damping, in some instances, was completely negated by the presence of the horizontal tail. This interference phenomenon was crudely illustrated by testing with the right horizontal tail panel removed. Consequently, only the inboard or outboard panel was present when the model was rotated to the left ($-\Omega b/2V$) or right, respectively. Figure 15 shows that the inboard panel alone approximates the horizontal tail-off configuration, whereas the outboard panel by itself approaches the horizontal tail-on configuration. It is indicated that the pressure field associated with the outboard horizontal tail is mainly responsible for the loss of vertical tail effectiveness in the flat spin.

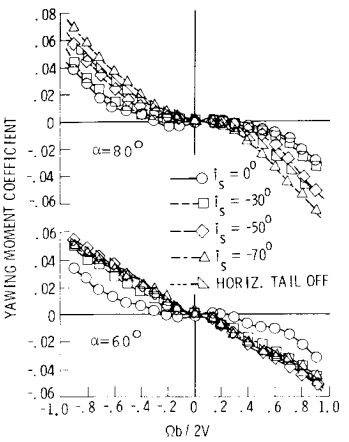

Fig. 16 Effect of indexing horizontal tail on yawing moment characteristic for model C.

Table 1 Experimental vs predicted spin characteristics[a] for model A

	α, deg	Ω, s/turn	$\Omega b/2V$
Spin model	38	2.5	0.22
tests	77	1.1	0.83
Steady-state	38	2.2	0.23
analysis	77	1.2	0.81

[a] Two spin modes.

Obviously, if one can unload the outboard panel by some means, such as reindexing the horizontal tail, the interference of the horizontal tail would be eliminated. This is shown to be the case in Fig. 16, which presents the yawing moment characteristics for various nose down horizontal tail deflections. At an α of 60 deg, an i_s value of only -30 deg approximated the horizontal tail-off characteristics. However, a deflection of the order of -60 deg is required at an α of 80 deg.

Application of Rotary Balance Testing to Specific Airplane Designs

Beside the use of the rotary balance apparatus for research investigations, it is also useful in the development of a specific configuration. The influence of various configuration components on the incipient and developed spin, as well as recovery characteristics, can be rapidly determined by inspection of the on-line rotary balance data. Also, on-line steady-state spin equilibrium conditions can be predicted.[14,15] (Off-line, the rotary balance data can be used to compute time histories of large angle motions employing an appropriate six-degree-of-freedom computer program.) It is possible, therefore, for the designer to develop a configuration that is highly resistant to spins, or one that has good spin recovery characteristics, if it is to be used for acrobatic maneuvers or training.

A closed-loop type of rotary balance spin model testing procedure, as opposed solely to spin model tests,[16] is now practicable since, as shown in Table 1, the correlation between spin model and predicted spin characteristics is quite acceptable. This procedure results in an appreciable reduction in spin model testing time.

Concluding Remarks

A rotary balance apparatus has been developed which rapidly identifies configuration aerodynamic characteristics in a rotational flow environment. A large data base can now be efficiently generated to permit a thorough understanding of the spin phenomenon and the development of design charts. It was demonstrated herein that there is a pronounced nonlinear dependency of the aerodynamic moments on rotational rate, and that these moment characteristics are very configuration dependent. For instance, it was shown that fuselage shape and horizontal tail location can be critically important in determining the existence of a flat spin mode.

The usefulness of the rotary balance extends beyond general research investigations; it can also be employed to develop a specific configuration highly resistant to spins, or one which has good spin and recovery characteristics. Also, the availability of rotary balance data reduces required spin tunnel and/or radio-control model testing time.

References

[1] Irving, H.B. and Batson, A.S., "Experiments on a Model of a Single Seater Fighter Aeroplane in Connection with Spinning," British Aeronautical Research Council, R&M No. 1184, May 1928.

[2] Bamber, M.J. and Zimmerman, C.H., "The Aerodynamic Forces and Moments Exerted on a Spinning Model of the 'NY-1' Airplane as Measured by the Spinning Balance," NACA Report 456, 1933.

[3] Stone, R.W. Jr., Burk, S.M. Jr., and Bihrle, W. Jr., "The Aerodynamic Forces and Moments of a 1/10-Scale Model of a Fighter Airplane in Spinning Attitudes as Measured on a Rotary Balance in the Langley 20-Foot Free Spinning Tunnel," NACA TN 2181, Sept. 1950.

[4] Bihrle, W. Jr. and Barnhart B., "Effects of Several Factors on Theoretical Predictions of Airplane Spin Characteristics," NACA CR 132521, Aug. 1974.

[5] Bihrle, W. Jr., "Correlation Study of Theoretical and Experimental Results for Spin Tests of a 1/10-Scale Radio Control Model," NASA CR 144995, July 1976.

[6] Bihrle, W. Jr., Hultberg, R.S., and Mulcay, W., "Rotary Balance Data for a Typical Single-Engine Low-Wing General Aviation Design for an Angle-of-Attack Range of 30° to 90°," NASA CR 2972, July 1978.

[7] Bihrle, W. Jr. and Hultberg, R.S., "Rotary Balance Data for a Typical Single-Engine General Aviation Design for an Angle-of-Attack Range of 8° to 90°, I—High Wing Model B," NASA CR 3097, Sept. 1979.

[8] Bihrle, W. Jr. and Hultberg, R.S., "Rotary Balance Data for a Typical Single-Engine General Aviation Design for an Angle-of-Attack Range of 8° to 90°, II—Low-Wing Model B," NASA CR 3098, Sept. 1979.

[9] Hultberg, R.S. and Mulcay, W., "Rotary Balance Data for a Typical Single-Engine General Aviation Design for an Angle-of-Attack Range of 8° to 90°, I—Low-Wing Model A," NASA CR 3100, Feb. 1980.

[10] Mulcay, W. and Rose, R., "Rotary Balance Data for a Typical Single-Engine General Aviation Design for an Angle-of-Attack Range of 8° to 90°, II—High-Wing Model A," NASA CR 3101, Sept. 1979.

[11] Bihrle, W. Jr. and Mulcay, W., "Rotary Balance Data for a Typical Single-Engine General Aviation Design for an Angle-of-Attack Range of 8° to 35°, III—Effect of Wing Leading-Edge Modifications Model A," NASA CR 3102, Nov. 1979.

[12] Mulcay, W. and Rose, R., "Rotary Balance Data for a Typical Single-Engine General Aviation Design for an Angle-of-Attack Range of 8° to 90°, I—Low-Wing Model C," NASA CR 3200, Oct. 1980.

[13] Hultberg, R.S., Chu, J., and Dickens, W., "Rotary Balance Data for a Typical Single-Engine General Aviation Design for an Angle-of-Attack Range of 8° to 90°, II—High-Wing Model C," NASA CR 3201, Oct. 1980.

[14] Babister, A.W., *Aircraft Stability and Control,* Vol. 1, Pergamon Press, New York, 1961, Chap. 16, p. 537.

[15] Bihrle, W. Jr. and Barnhart, B., "Spin Prediction Techniques," AIAA Paper 80-1564-CP, Aug. 1980.

[16] Burk, S.M. Jr., Bowman, J.S. Jr., and White, W.L., "Spin-Tunnel Investigation of the Spinning Characteristics of Typical Single-Engine General Aviation Airplane Designs, I—Low-Wing Model A, Effects of Tail Configurations," NASA TP 1009, Sept. 1977.